

Dependence of sensitivity of SnO_x thin-film gas sensors on vacancy defects

Cite as: Journal of Applied Physics **80**, 6050 (1996); <https://doi.org/10.1063/1.363562>

Submitted: 12 December 1995 • Accepted: 16 August 1996 • Published Online: 17 August 1998

D. S. Vlachos, C. A. Papadopoulos and J. N. Avaritsiotis



View Online



Export Citation

ARTICLES YOU MAY BE INTERESTED IN

Gas sensing in 2D materials

Applied Physics Reviews **4**, 021304 (2017); <https://doi.org/10.1063/1.4983310>

Resistive gas sensors based on metal-oxide nanowires

Journal of Applied Physics **126**, 241102 (2019); <https://doi.org/10.1063/1.5118805>

Microstructure, optical, and electrical properties of *p*-type SnO thin films

Applied Physics Letters **96**, 042113 (2010); <https://doi.org/10.1063/1.3277153>

Journal of Applied Physics **Special Topics** Open for Submissions [Learn More](#)

Dependence of sensitivity of SnO_x thin-film gas sensors on vacancy defects

D. S. Vlachos, C. A. Papadopoulos, and J. N. Avaritsiotis^{a)}

Department of Electrical and Computer Engineering, Division of Computer Science, National Technical University of Athens, 157 73 Zographou, Athens, Greece

(Received 12 December 1995; accepted for publication 16 August 1996)

Oxygen flow during dc reactive sputtering of SnO_x thin films affects film conductivity in zero grade air and gas sensitivity to carbon monoxide and ethanol. The experimental results show that an increase in oxygen flow during film deposition produces films exhibiting higher conductivity in zero grade air and lower gas sensitivity. A theoretical model is presented that explains this behavior. The proposed model takes into account both the dependence of conductivity on the potential barrier height at grain boundaries of the film and the dependence of chemisorption rate of oxygen on free-electron availability. The theoretical analysis is in good qualitative agreement with experiment.

© 1996 American Institute of Physics. [S0021-8979(96)05122-5]

I. INTRODUCTION

Tin oxide films are used as gas sensors due to their high sensitivity. In the presence of small amounts of some gases of interest, such as carbon monoxide, ethanol, and methane the film conductance changes.¹ Tin oxide is a wide band gap (3.6 eV) *n*-type semiconductor, whose conductivity depends upon oxygen vacancies.² The conductance of SnO_x films may be altered by changes in film stoichiometry. The presence of oxidizing gases decreases film conductance, whereas the presence of reducing gases increases it.³ Therefore, the presence of reducing gases in the ambient air can be sensed via the effect they have on the conductance of the film (resistive type gas sensors). The range of applications of this type gas sensors is limited by the poor selectivity they have.⁴ Efforts to enhance the selectivity have been focused on the addition of catalysts, promoters and filters on the SnO_x film.⁵ As the principles of catalysis are not yet well understood, the problem has not been yet solved, although some progress has been made.

The need of sensors with various characteristics for applications in sophisticated systems such as neural networks, motivates the design of sensors with various stoichiometries. One way to obtain this is to control the O:Sn ratio in tin oxide thin films by varying the oxygen flow during reactive sputtering deposition. Since the amount of oxygen vacancies in tin oxide film is the main electron donor, the conductivity of these films may be used to monitor the film stoichiometry.

In this work, the conductivity of tin oxide thin films produced by reactive dc sputtering in various oxygen flows is studied in zero grade air as well as in CO and ethanol ambient. A theoretical model is proposed to explain the experimental results for both the conductivity and the sensitivity of these films.

II. EXPERIMENTAL TECHNIQUES

Deposition of SnO_x films was performed with a Leybold Z-400 planar magnetron sputtering system, which was dc operated in a controlled, high-purity Ar-O₂ mixture. Two

different discharge modes may be obtained, the metallic mode and the reactive mode, where the target is respectively free from or covered with reaction products. The compound formation reactions are desirable in the metallic mode for high rate depositions, and for a more precise control of the O₂/Sn ratio of the deposited film. This necessitates the use of a plasma emission monitor (PEM) system, that allows us to select and maintain the degree of target oxidation,⁶ with the tin emission line intensity at 450 nm as a measurand for the control loop of the reactive gas mass flow controller.

Films were fabricated at a relatively high total gas pressure of approximately 1.0×10^{-2} mbar. The substrate holder was at a distance of 7 cm from the 10 cm-in-diameter target. The total power into the tin target (99.99%) was 115 W with a total current of 0.36 A, thus achieving a deposition rate of approximately 100 nm/min. The argon flow was adjusted manually at 20 ml/min, while the oxygen intake was controlled by the aforementioned PEM control unit, so that the intensity of the tin emission line remained constant.

By varying deposition temperature and pressure we can control film structure. Density and crystallite size increase with temperature. At a deposition temperature of 460 °C low density films (43% single crystal) with a medium crystallite size (11 nm) and a high specific area (50 m²/g) are produced.⁷ This structure is suitable to obtain better sensitivity, but the mechanical properties of the film depend on the density in opposite direction to the sensitivity. For higher deposition temperatures (560 °C), the microstructure becomes more dense (85% single crystal) with a larger crystallite size (30 nm) and a lower specific area (15 m²/g). A scanning electron micrograph of such a sample shows a fine modular microstructure with spherical grains. The total pressure during deposition is known to affect film structure.⁸ Films are compact for total pressure less than 5×10^{-2} mbar, become columnar for pressures up to 0.8 mbar and become spongy for pressure higher than 0.8 mbar.

The deposition of our films was carried out on Al₂O₃ substrate with dimensions 12×26 mm, heated at 300 °C. At this temperature the film consists mainly of [110] crystallites. Crystallinity and morphology of the SnO_x films were studied by x-ray diffraction (XRD) and scanning electron micros-

^{a)}Electronic mail: abari@cs.ntua.gr

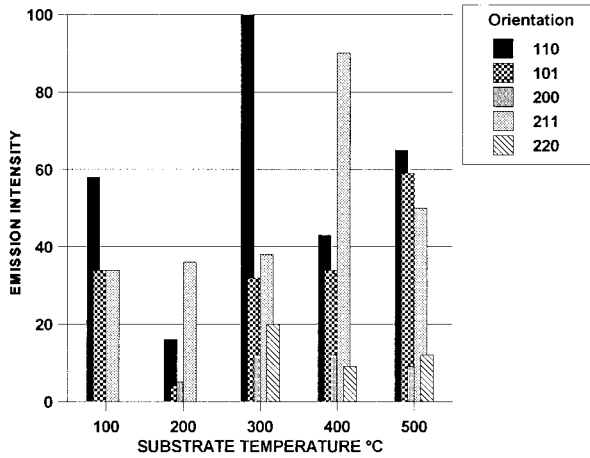


FIG. 1. Crystal structure vs substrate temperature during film deposition.

copy. The results are summarized in Fig. 1. As shown in Fig. 1, the deposited films are composed of crystallites with [110], [101], [200], [211], [220] orientations. The XRD analysis shows that the orientation [110] dominates if the substrate temperature is around 300 °C during deposition.

Film dimensions were 1.2×2.0 mm approximately, obtained using a metal contact mask. The mask was cleaned in HCl solution each time before sputtering, in order to remove SnO_x remains from previous deposition runs. The films were fabricated with a constant Ar flow of 20.0 ml/min and a variable O₂ flow, in order to achieve different oxygen to tin ratio in each film. Oxygen flow was varied from 24 to 45 ml/min, so oxygen to tin ratio was varied from 1.2 to 2.25. If O₂/Sn ratio is low, the films have a metallic composition and cannot function as gas sensors; if O₂/Sn ratio is relatively high, the fabricated films are highly resistive (small concentration of oxygen vacancies) and again cannot function as sensors. The sputtering system was operated in constant current mode. The thickness of all films fabricated was equal to 2000 nm (20 min sputtering time).

The sensor characterization setup was designed to measure the steady state and the transient response of the samples, testing them under various temperatures and ambient gases. The testing conditions are rigorously controlled via a fully automated, computer controlled system. All sensors have been characterized according to the following experimental procedure:

- (i) The samples were heated to 450 °C and cooled back to 150 °C in zero grade air. This step was repeated three times before starting film characterization, in order to clean the samples from water vapor remains.
- (ii) The samples were heated to 450 °C in zero grade air. Then CO was introduced in the chamber with concentration of 2650 ppm, and the samples were cooled back to 150 °C.
- (iii) The samples were heated to 450 °C and cooled back to 150 °C in zero grade air.
- (iv) Step (ii) was repeated but with a test gas composition of 30 ppm ethanol in zero grade air instead of CO.
- (v) Step (iii) was repeated.

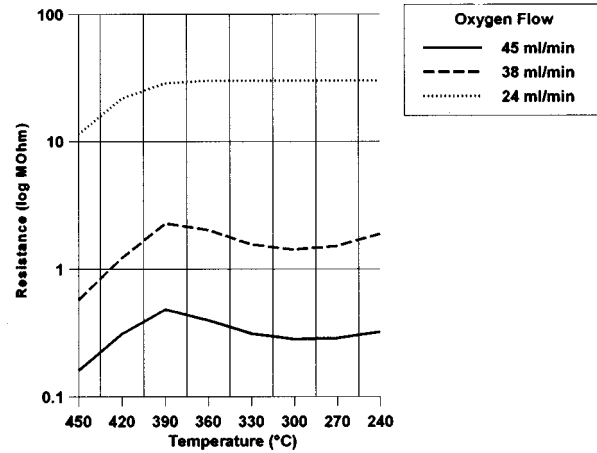


FIG. 2. Experimental results showing the resistance of films prepared at different oxygen mass flow values against working temperature.

During the aforementioned measuring cycles, the resistance of the samples was recorded at 5 °C intervals as the samples were cooled from 450 to 150 °C. The cooling speed was 10 °C/min. At temperatures above 250 °C, such a speed ensures that no significant transient effects occur.⁹

III. EXPERIMENTAL RESULTS AND DISCUSSION

The conductivity against temperature in zero grade air is shown in Fig. 2 for three samples prepared with different oxygen flows. It is apparent that the conductivity of the samples increases with increasing film oxygen content. These results seem to be contradictory, because it is known that oxygen vacancies in tin oxide act as electron donors¹⁰ and thus they tend to increase the conductivity of the film. The number of oxygen vacancies is expected to increase in low oxygen flows during the film deposition. We will show that such an effect may be expected in the case of either small grain size films or films with high O:Sn ratio.

At a first approximation, the intergranular conductance G of SnO_x films at a temperature T may be described¹¹ by Eq. (1)

$$G = G_0 n_0 R e^{-\psi_s}, \quad (1)$$

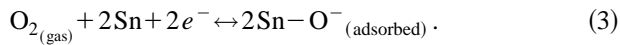
where n_0 is the electron concentration in flat-band condition, G_0 is a factor which includes charge and mobility of carriers and geometrical effects, $\psi_s = \beta \Delta y_s$ is the dimensionless band bending at grain surface, R represents band bending at the center of the grain (considered as an offset) and the term

$$\frac{1}{\beta} (\psi_s - \ln R) \quad (2)$$

is the Schottky barrier y_s . The transformation to dimensionless form is obtained by the following way: If y_s is the bending of the semiconductor energy bands at the surface, then it is assumed that $y_s = y_0 + \Delta y_s$, where y_0 is constant so that Δy_s is zero at the centre of the grain. Then R is the term $\exp(-\beta y_0)$ and ψ_s is the term $\beta \Delta y_s$. The voltage drop at each intergranular contact has been assumed to be less than $1/\beta = kT/q$ so that voltage dependence of current is ohmic²

for the voltages applied to the sample. Under real atmospheric conditions the barrier energy is a function of temperature T , oxygen partial pressure and the partial pressures of other reducing or oxidizing gases. Equation (1) is applicable to the temperature range where the concentration of ionized donors is approximately independent of temperature. It is worth noting that native donor levels of 0.03–0.034 eV and 0.14–0.15 eV below the conduction band edge in n -type tin dioxide¹¹ are generally thought to result from the single and double ionization of oxygen vacancies.

Film conductivity increases with increasing free-electron concentration. But, according to the kinetics of the chemisorption of oxygen on tin oxide, the increasing concentration of free electrons favors the generation of oxygen adatoms according to Eq. (3):



It is apparent that the rate of chemisorption is proportional to the second power of electron concentration. The increase in the free-electron concentration is expected to decrease the bending of the semiconductor near the surface. Consequently, assuming that the oxygen adatoms introduce a single-energy level (acceptor like surface states) in the band gap of the semiconductor, more electrons can occupy these states, resulting to an increase in the concentration of oxygen adatoms with the synchronous decrease in free-electron density.

The maximum number of the aforementioned acceptor states is the Weisz limit.¹² This is the maximum number of adsorbed oxygen atoms which is obtained by taking into account electrostatic interactions. The occupation of these states follows the Fermi–Dirac statistics.¹³ Assuming that a grain is represented by a infinite layer between $x = -W/2$ and $x = W/2$, the dimensionless Poisson equation gives

$$\frac{d^2\psi}{dz^2} = 1 - Re^{-\psi},$$

where $z = \lambda x$, $\psi = \beta y$, $\lambda = \sqrt{(qn_0\beta)/\epsilon_s}$, (4)

where ϵ_s is the dielectric constant and y is the bending of the semiconductor without the constant offset [see Eq. (2)]

$$y_0 = -\frac{1}{\beta} \ln R. \quad (5)$$

The charge conservation gives the condition necessary to solve Eq. (4):

$$\left. \frac{d\psi}{dz} \right|_{z=\lambda(W/2)} = \frac{q\beta N}{\lambda\epsilon_s}, \quad (6)$$

where N is the density of occupied acceptors states and, according to Fermi–Dirac statistics,¹³ it is equal to

$$N = N_0 \frac{1}{1 + (X/R)e^{\psi_s}}. \quad (7)$$

The constant parameters N_0 and X incorporate the Weisz limit and the energy level of the acceptor states, respectively.

Since the dimensionless bending ψ is considered to have an offset it must be zero at $z=0$. Moreover, due to symmetry, $d\psi(0)/dz=0$ also. An approximate solution for ψ is

$$\psi(z) = \frac{N}{n_0} \frac{z^2}{W}. \quad (8)$$

By integrating Eq. (4) from $\psi=0$ to $\psi=\psi_s=\psi(\lambda W/2)$, we have

$$\frac{1}{2} \left(\left. \frac{d\psi}{dz} \right|_{z=\lambda(w/2)} \right)^2 = \psi_s - R(1 - e^{-\psi_s}), \quad (9)$$

where ψ_s is the dimensionless bending at the surface. Replacing in Eq. (9) the dimensionless surface bending ψ_s from Eq. (8) and with the help of Eq. (6), we obtain

$$\frac{1}{2} \frac{qN^2\beta}{n_0\epsilon_s} = \frac{qN\beta}{\epsilon_s} \frac{W}{4} - R(1 - e^{-\psi_s}). \quad (10)$$

As it was mentioned above, the oxygen flow during film deposition affects oxygen vacancies density and thus the free electron concentration. The dependence of film conductivity on vacancy concentration then can be obtained by replacing in Eq. (1) the offset R from Eq. (7) and taking the derivative over n_0 :

$$\frac{dG/dn_0}{G} = \frac{1}{n_0} + \frac{N_0}{N} \frac{1}{N_0 - N} \frac{dN}{dn_0}. \quad (11)$$

In the case of small grain or low number of free electrons (i.e., the case with high O:Sn ratio), we may assume that all the electrons move to the surface states, i.e.,

$$n_0W = 2N. \quad (12)$$

Then, calculating dN/dn_0 from Eq. (10) and substituting in Eq. (11), we obtain

$$\frac{dG/dn_0}{G} = -\frac{N}{n_0(N_0 - N)}. \quad (13)$$

Equation (13) means that an increase of free-electron concentration will induce a decrease in the conductivity when and only when Eq. (12) holds. As shown in Fig. 2, this result is applicable over the whole temperature range of the experiment, i.e., the resistance increases with increasing free-electron concentration. The sigmoid-like shape of resistance is caused by the doubly ionization of oxygen adatoms.¹⁴ At relatively low temperatures (below 300 °C), the resistance behaves like in semiconductors. At this point, doubly ionization of oxygen adatoms increases the number of surface states and the resistance increases too. Above 390 °C this process saturates and the resistance again behaves like that of a typical semiconductor.

The gas sensitivity now may be expressed as the change in conductivity over the change in surface electron states. Reducing gases like CO remove oxygen adatoms which results in a decrease of the number of occupied surface states induced by oxygen chemisorption. Therefore, the sensitivity S is given

$$S = \frac{dG/dN_0}{G}. \quad (14)$$

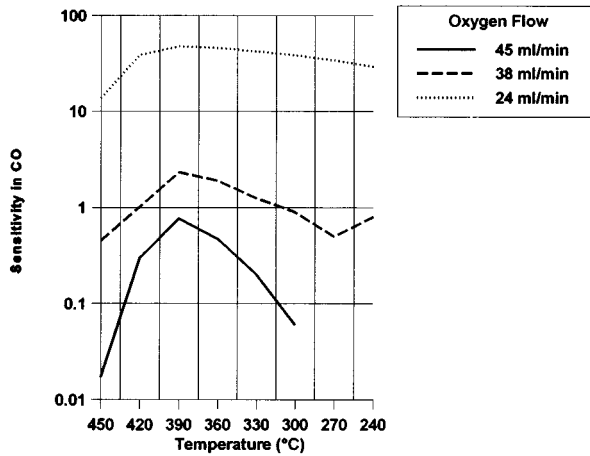


FIG. 3. Experimental results showing the sensitivity of films prepared at different oxygen mass flow values against working temperature, in the presence of 2650 ppm CO.

The effect of oxygen vacancies on sensitivity can be calculated now by considering the change in sensitivity over the change in oxygen vacancies (or free-electron concentration). Taking the derivative of Eq. (14) over n_0 in the case of small grain size or of low electron concentration, we obtain

$$\frac{dS}{dn_0} = \frac{1}{(N_0 - N)^2} \frac{N}{n_0}. \quad (15)$$

Equation (15) means that the sensitivity increases with increasing electron concentration. Figure 3 shows the experimental results for the gas sensitivity in 2650 ppm CO. The sensitivity of the film increases with decreasing oxygen flow during deposition (i.e., increasing free-electron concentration) as it was found in Eq. (15) over the whole temperature range of the experiment. The sensitivity exhibits a maximum at a temperature close to 390 °C, where it is believed that the surface state density is maximum due to the doubly ionization of oxygen adatoms. Consequently, the reaction of CO molecules with oxygen adatoms which leads to the formation of CO₂, returns to the crystal two electrons. At lower temperatures, the same reaction returns to the crystal one electron since the oxygen adatoms are singly ionized. At temperatures above 390 °C where the ionization of oxygen adatoms saturates, the sensitivity decreases because the resistance of the film decreases due to thermal generated electrons. Figure 4 shows the experimental results for the sensitivity in 30 ppm ethanol. Again, Eq. (15) is applicable but different mechanism of interaction between ethanol and tin oxide has to be considered. Ethanol molecules adsorb on tin atoms, while adsorbed ethanol molecules dissociate and act as electron donors with the aid of adsorbed oxygen atoms.³ Thus, there will be an optimum Sn:O ratio in which ethanol exhibits maximum sensitivity. This can be observed in Fig. 4, where as oxygen vacancies increase (45–38 ml/min oxygen flow during deposition) the sensitivity increases, while further increase of oxygen vacancies (38–24 ml/min oxygen flow during deposition) tends to decrease the sensitivity. Again, doubly ionization of oxygen adatoms cause a maxi-

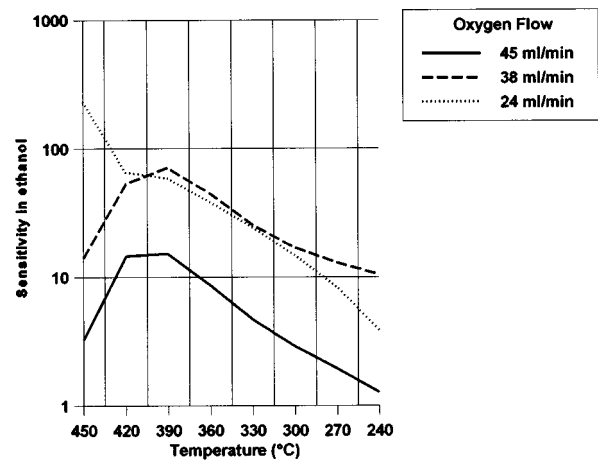


FIG. 4. Experimental results showing the sensitivity of films prepared at different oxygen mass flow values against working temperature, in the presence of 30 ppm ethanol.

imum to sensitivity at 390 °C as in the case of CO. As for the experimental curve of sensitivity of the film deposited with oxygen flow 24 ml/min, which does not exhibit this maximum, it is believed that one has to consider not only the electronic but the chemical interaction of ethanol with tin oxide surface as well.¹⁴

IV. CONCLUSIONS

The effect of oxygen flow during dc reactive sputtering of SnO_x thin films on film conductivity and gas sensitivity was studied. Oxygen flow is considered to affect film stoichiometry and thus free-electron concentration. More specifically, by increasing the oxygen flow, the O:Sn ratio and thus the number of oxygen vacancies is expected to decrease. Since these vacancies are the electron donors in the *n*-type SnO_x semiconductor, the free-electron concentration is expected to decrease too.

Moreover, given that the chemisorption of oxygen atoms on tin oxide surface takes place by electron transfer from the film to the chemisorbed atoms, a decrease of free electron concentration is expected (due to high O:Sn ratio or relatively small grain size) to induce an increase of film conductivity. It has also been proved that by increasing the oxygen flow during sputtering, the number of chemisorbed oxygen and consequently the sensitivity of the film is decreased.

¹M. J. Willett, in *Techniques and Mechanisms in Gas Sensing*, edited by P. T. Moseley, J. O. W. Norris, and D. E. Williams (Adam Hilger, Bristol, 1991), Chap. 3, pp. 61–105.

²V. Lantto, P. Romppainen, and S. Leppavuori, *Sens. Actuators B* **14**, 149 (1988).

³D. Kohl, *Sens. Actuators* **18**, 71 (1989).

⁴D. Kohl, *Sens. Actuators B* **1**, 158 (1990).

⁵S. R. Morrison, *Sens. Actuators* **12**, 425 (1987).

⁶C. D. Tsiogas and J. N. Avaritsiotis, *Vacuum* **45**, 1181 (1994).

⁷B. Gautheron, M. Labeau, G. Delabouglise, and U. Schmatz, *Sens. Actuators B* **15–16**, 357 (1993).

⁸C. Pijolat, P. Breuil, A. Methivier, and R. Lalauze, *Sens. Actuators B* **13–14**, 646 (1993).

- ⁹P. D. Skafidas, D. S. Vlachos, and J. N. Avaritsiotis, *Sens. Actuators B* **21**, 109 (1994).
- ¹⁰J. Robertson, *Phys. Rev. B* **30**, 3520 (1984).
- ¹¹V. Lantto and P. Romppainen, *Surf. Sci.* **192**, 243 (1987).
- ¹²P. B. Weisz, *J. Chem. Phys.* **21**, 1531 (1953).
- ¹³S. M. Sze, *Physics of Semiconductor Devices*, 2nd ed. (Wiley, New York, 1981), Chap. 1, p. 17.
- ¹⁴P. T. Moseley and D. E. Williams, in *Techniques and Mechanisms in Gas Sensing*, edited by P. T. Moseley, J. O. W. Norris, and D. E. Williams (Adam Hilger, Bristol, 1991), Chap. 2, pp. 46–60.